

# Efficient Sensor Management for Multitarget Tracking in Passive Sensor Networks via Cauchy-Schwarz Divergence

Yun Zhu

**Abstract**—This paper presents an efficient sensor management approach for multi-target tracking in passive sensor networks. Compared with active sensor networks, passive sensor networks have larger uncertainty due to the nature of passive sensing. Multi-target tracking in passive sensor networks is challenging because the multi-sensor multi-target fusion problem is difficult and sensor management is necessary to achieve good trade-offs between tracking accuracy and energy consumption or other costs. To address this problem, we present an efficient information-theoretic approach to manage the sensors for better tracking of the unknown and time-varying number of targets. This is accomplished with two main technical innovations. The first is a tractable information-based multi-sensor selection solution via a partially observed Markov decision process framework. The Cauchy-Schwarz divergence is used as the criterion to select informative sensors sequentially from the candidates. The second is a novel dual-stage fusion strategy based on the iterated-corrector multi-sensor generalized labeled multi-Bernoulli filter. Since the performance of the iterated-corrector scheme is greatly influenced by the order of sensor updates, the selected sensors are first ranked in order of their abilities to detect targets according to the Cauchy-Schwarz divergence, followed the iterated-corrector update. The computation costs of ranking the sensors are negligible, since the Cauchy-Schwarz divergence has been computed in the multi-sensor selection procedure. Simulation results validate the effectiveness and efficiency of the proposed approach.

**Index Terms**—Multi-target tracking; random finite set; generalized labeled multi-Bernoulli; sensor network; Doppler measurements.

## I. INTRODUCTION

**S**ENSOR networks composed of moving robots or static sensing nodes have attracted attentions in various fields, such as surveillance, scene analysis, and so forth. Multi-sensor multi-target tracking, one of the most critical low-level techniques, is difficult in twofold. On the one hand, multi-sensor fusion for multi-target tracking is challenging due to data association uncertainty between measurements and targets. On the other hand, intelligent sensor management is required to report high quality target-related measurements, with a view to provide a balance in tracking accuracy and energy consumption of the sensor network [1], [2]. Embedded in highly complex multi-target systems, sensor management is inherently an optimal nonlinear stochastic control problem and standard optimal control techniques are not directly applicable.

A unified approach to addressing the stochastic nature of the multi-target sensor management is a Bayesian paradigm in which uncertainty is represented by multi-target probability density functions in a systematic manner using finite set statistics (FISST) [3]. The (cardinalized) probability hypothesis density (PHD) [4], [5] and the multi-Bernoulli [6] filters are popular approaches within the FISST framework. These filters are crude approximations to the Bayes multi-target filter and were not explicitly designed to estimate target trajectories. The most advanced FISST-based algorithm, known as the generalized labeled multi-Bernoulli (GLMB) filter is an analytic solution to the Bayes multi-target filter that explicitly produces target tracks [7], [8]. The GLMB filter can be implemented with linear complexity in the number of measurements using Gibbs sampling [9] and has been demonstrated to be the most efficient, handling in excess of one million tracks simultaneously from over a billion measurements [10]. Moreover, the GLMB approach also admits multi-sensor multi-target solutions that are linear in the sum of the measurements [11], as well as multi-scan solutions that are linear in the number of scans [12]. What distinguishes the GLMB family from other multi-target filters is that their approximation errors can be captured analytically [8].

Within the FISST framework, sensor management is treated as an optimization problem that yields the best sensor control action. Objective functions proposed for sensor management were mainly task-based and information measures. Task-based sensor management includes minimization of the cardinality variance [13], [14], minimization of statistical mean of the optimal sub-pattern assignment (OSPA) error [15], maximization of the posterior expected number of targets [16], [17], [18]. One can design a “task-driven” sensor management strategy that addresses one of these tasks but it may be poor in addressing the others. Ad hoc methods that address several tasks by assigning relative weight to each task can also be used [19], [20], [21]. However, this requires one to assign relative values to each task. Our recent work [22] considers the legacy tracks and measurement-updated tracks separately, to make full use of information involved in the multi-target posterior density. To deal with a multitude of performance criteria in a direct manner simultaneously, some researchers have proposed to use information theoretic measures as objective or reward functions. In the context of Bayesian estimation, a principled measure of information gain is the divergence between the predicted and updated multi-target densities, and divergences such as Kullback-Leibler [23], and Rényi [24] have been

Yun Zhu is with the Key Laboratory of Modern Teaching Technology, Ministry of Education, and the School of Computer Science, Shaanxi Normal University, Xi'an City, Shaanxi Province, China.

widely used. However, these divergences cannot be computed analytically. In [25] and [26], the authors derived closed form Cauchy-Schwarz divergences for Poisson and GLMB models, providing additional tools to tackle complex problems in multi-target systems. A special case of this GLMB sensor management approach has been applied to drone path-planning [27]. Multi-objective path-planning for multiple agents with competing objectives has also been developed in [28].

Regardless of the objective function, sensor management is essentially a global combinatorial optimization problem that is extremely challenging when the sensor network is large (except for the special case where only one sensor is selected). To alleviate this computational issue, a spatial non-maximum suppression heuristics was developed in [29], which requires tuning the parameter of the suppress gate. A suboptimal solution was proposed in [30], but it is not suitable for the sensor selection problem. A subselection problem for each target was investigated in [31], and it was solved by maximizing the information gain of the PHD filter. In this method, the number of activated sensors is out of the user's control and hence the system may not meet the communication and real-time constraints.

In this paper, we consider the sensor management problem for multi-target tracking in passive sensor networks. Compared with active sensors, the use of passive sensors is attractive since they cost less and are robust in extreme environments. At each time step, receivers in the passive sensor network send their observations regarding the multi-target state to a central node called the fusion center, which is responsible for the final inference. However, since transmit and receive antennas are placed at different locations, measurements collected by passive sensor networks are typically subjected to noise corruption, missed detections, and false alarms. Worse, the detection ability of the passive sensor network deteriorates severely as the distance from the receiver increases. To deal with these challenges, we adopt the iterated-corrector multi-sensor GLMB filter as a centralized fusion scheme and develop an efficient sensor management solution. The main contributions are as follows.

First, a novel information-theoretic multi-sensor selection approach based on the Cauchy-Schwarz divergence is proposed. Typically, a passive sensor network is realized with either one receiver and multiple transmitters or a single transmitter combined with multiple receivers. Due to communication and real-time constraints, the system may need to select a subset of sensors to report high quality target-related measurements. In this paper, we adopt the iterated-corrector multi-sensor GLMB filter as a centralized fusion scheme and develop an efficient multi-sensor selection solution under the framework of partially observed Markov decision process (POMDP). A tractable solution is proposed via sequential selection of the best from the candidates, based on the Cauchy-Schwarz divergence between the prior and posterior GLMB densities. This approach is efficient since it is not necessary to search over all possible sensor combinations and the Cauchy-Schwarz divergence for GLMBs admits a closed form expression [26].

Second, an improved fusion strategy with a modified update

is proposed. As mentioned above, the iterated-corrector multi-sensor GLMB filter is used as the fusion scheme, which has simple practical implementation. However, a well-known drawback of the iterated-corrector update is that it results in different filtering densities depending on the order of the sensor updates. If the detection ability of the last sensor is low, the overall performance of the filter degrades. To deal with this, we propose a dual-stage iterated-corrector update method. Firstly, the sensors are ranked according to their abilities to detect targets based on the Cauchy-Schwarz divergence. The computation involved in this procedure is negligible, since the Cauchy-Schwarz divergence has been evaluated in the previous multi-sensor selection. Secondly, the iterated-corrector update is applied in order of the ranking. The multi-target density is updated by the sensor with weak detection ability first, and then the sensor with better detection performance is used in turn.

The paper is organized as follows. In Section 2, the necessary background on GLMB recursion is presented and the multi-static passive radar network is briefly introduced. In Section 3, the proposed approach with efficient multi-sensor selection and dual-stage iterated-corrector update is presented in detailed. In Section 4, numerical studies are given. Finally, Section 5 concludes the paper.

## II. PROBLEM FORMULATION

### A. Labeled RFS

In the FISST framework, the target states take values from a state space  $\mathbb{X}$ . The multi-target state space is the space of all finite subsets of  $\mathbb{X}$  and is denoted as  $\mathcal{F}(\mathbb{X})$ . A multi-target state at each time is modelled as a random finite set (RFS), a random variable that take values from  $\mathcal{F}(\mathbb{X})$ . To address target trajectories in the FISST framework in a principled manner, the simplest approach is to incorporate labels into the multi-target state to identify individual targets [3]. A label  $\ell \in \mathbb{L}$  is augmented to the state of each target and the multi-target state is considered as a finite set on  $\mathbb{X} \times \mathbb{L}$ . Since some targets may share the same identity, we require that the RFS modelling the multi-target state on  $\mathbb{X} \times \mathbb{L}$  have distinct labels [3]. This is the essence of labeled RFS, i.e. marked RFS with discrete and distinct marks [7], [8]. By convention, single-target states are represented by lowercase letters, e.g.,  $x$ ,  $\mathbf{x}$ , while multi-target states are represented by uppercase letters, e.g.,  $X$ ,  $\mathbf{X}$ . Symbols for labeled states and their distributions are bolded to distinguish them from unlabeled ones, e.g.,  $\mathbf{x}$ ,  $\mathbf{X}$ , etc.

Suppose that at time  $k$ , there are  $N(k)$  target states  $\mathbf{x}_{k,1}, \dots, \mathbf{x}_{k,N(k)}$  each taking values in a labeled state space  $\mathbb{X} \times \mathbb{L}$ , and  $M(k)$  measurements  $z_{k,1}, \dots, z_{k,M(k)}$ , each taking values in an observation space  $\mathbb{Z}$ . The set of target states and measurements are treated as the multi-target state and multi-target measurement, respectively

$$\mathbf{X}_k = \{\mathbf{x}_{k,1}, \dots, \mathbf{x}_{k,N(k)}\} \in \mathcal{F}(\mathbb{X} \times \mathbb{L}) \quad (1)$$

$$\mathbf{Z}_k = \{z_{k,1}, \dots, z_{k,M(k)}\} \in \mathcal{F}(\mathbb{Z}). \quad (2)$$

The multi-target Bayes recursion propagates the multi-target posterior density  $\pi_k(\mathbf{X}_k|Z_{1:k})$  in time according to the following update and prediction

$$\pi_k(\mathbf{X}_k|Z_{1:k}) = \frac{g_k(Z_k|\mathbf{X}_k)\pi_{k|k-1}(\mathbf{X}_k|Z_{1:k-1})}{\int g_k(Z_k|\mathbf{X})\pi_{k|k-1}(\mathbf{X}|Z_{1:k-1})\delta\mathbf{X}} \quad (3)$$

$$\pi_{k|k-1}(\mathbf{X}_k|Z_{1:k-1}) = \int \mathbf{f}_{k|k-1}(\mathbf{X}_k|\mathbf{X})\pi_{k-1}(\mathbf{X}|Z_{1:k-1})\delta\mathbf{X} \quad (4)$$

where  $\mathbf{f}_{k|k-1}(\cdot|\cdot)$  is the multi-target transition density that encapsulates the underlying models of target motions, births and deaths;  $g_k(\cdot|\cdot)$  is the multi-target likelihood that encapsulates detection uncertainty, clutter, data association uncertainty, and the usual observation noise. Note that the integrals in (3) and (4) are not ordinary integrals, but are set integrals. The set integral for a function  $f: \mathcal{F}(\mathbb{X} \times \mathbb{L}) \rightarrow \mathbb{R}$  is given by [7]

$$\int \mathbf{f}(\mathbf{X})\delta\mathbf{X} = \sum_{i=0}^{\infty} \frac{1}{i!} \int \mathbf{f}(\{\mathbf{x}_1, \dots, \mathbf{x}_i\})d(\mathbf{x}_1, \dots, \mathbf{x}_i). \quad (5)$$

The multi-target filtering density captures all information on the multi-target state, such as the number of targets and their states, at the current time.

Throughout the paper, we use the standard inner product notation

$$\langle f, g \rangle \triangleq \int f(x)g(x)dx \quad (6)$$

and the following multi-object exponential notation

$$h^{\mathbf{X}} \triangleq \prod_{x \in \mathbf{X}} h(x). \quad (7)$$

The inclusion function and the Kronecker delta function are given to support arbitrary arguments such as sets, vectors, and integers, as follows:

$$1_S(X) \triangleq \begin{cases} 1, & \text{if } X \subseteq S \\ 0, & \text{otherwise} \end{cases}, \quad \delta_S(X) \triangleq \begin{cases} 1, & \text{if } X = S \\ 0, & \text{otherwise} \end{cases}. \quad (8)$$

## B. Generalized Labeled Multi-Bernoulli

An important class of labeled RFS is the GLMB family [7], [8]. Under the standard multi-target model, the GLMB is a conjugate prior that is also closed under the Chapman-Kolmogorov equation. This means if we start with a GLMB initial prior, then the multi-target prediction and posterior densities at any time are also GLMB densities. Let  $\mathcal{L}(\mathbb{X} \times \mathbb{L}) \rightarrow \mathbb{L}$  be the projection  $\mathcal{L}(x, \ell) = \ell$  and  $\Delta(\mathbf{X}) \triangleq \delta_{|\mathbf{X}|}(|\mathcal{L}(\mathbf{X})|)$  denote the distinct label indicator. A GLMB is an RFS on  $\mathbb{X} \times \mathbb{L}$  distributed according to

$$\pi(\mathbf{X}) = \Delta(\mathbf{X}) \sum_{c \in \mathbb{C}} w^{(c)}(\mathcal{L}(\mathbf{X})) [p^{(c)}]^{\mathbf{X}} \quad (9)$$

where  $\mathbb{C}$  is a discrete index set,  $w^{(c)}(L)$  and  $p^{(c)}$  satisfy:

$$\sum_{L \subseteq \mathbb{L}} \sum_{c \in \mathbb{C}} w^{(c)}(L) = 1 \quad (10)$$

$$\int p^{(c)}(x, \ell) dx = 1. \quad (11)$$

The GLMB density (9) can be interpreted as a mixture of multi-target exponentials, where each term consists of a weight  $w^{(c)}(\mathcal{L}(\mathbf{X}))$  that depends only on the labels of  $\mathbf{X}$ , and a multi-target exponential  $[p^{(c)}]^{\mathbf{X}}$  that depends on the entire  $\mathbf{X}$ .

For implementation, it is easier to use the delta-form of the GLMB, known as  $\delta$ -GLMB [8]. In fact, a  $\delta$ -GLMB is a GLMB with

$$C = \mathcal{F}(\mathbb{L}) \times \Xi \quad (12)$$

$$w^{(c)}(L) = w^{(I, \xi)}(L) = w^{(I, \xi)} \delta_I(L) \quad (13)$$

$$p^{(c)} = p^{(I, \xi)} = p^{(\xi)} \quad (14)$$

where  $\Xi$  is a discrete space, i.e., it is distributed according to

$$\pi(\mathbf{X}) = \Delta(\mathbf{X}) \sum_{(I, \xi) \in \mathcal{F}(\mathbb{L}_+) \times \Xi} w_+^{(I, \xi)} \times \delta_{I_+}(\mathcal{L}(\mathbf{X}_+)) [p_+^{(\xi)}]^{\mathbf{X}_+}. \quad (15)$$

Clearly, the family of  $\delta$ -GLMB is also closed under the Chapman-Kolmogorov prediction and Bayes update. It was shown in [7] that if the multi-target prior is a  $\delta$ -GLMB with the form (15), the multi-target prediction is also a  $\delta$ -GLMB with the following form

$$\pi_+(\mathbf{X}_+) = \Delta(\mathbf{X}) \sum_{(I_+, \xi) \in \mathcal{F}(\mathbb{L}_+) \times \Xi} w_+^{(I_+, \xi)} \times \delta_{I_+}(\mathcal{L}(\mathbf{X}_+)) [p_+^{(\xi)}]^{\mathbf{X}_+} \quad (16)$$

where

$$w_+^{(I_+, \xi)} = w_B(I_+ \cap \mathbb{B}) w_S^{(\xi)}(I_+ \cap \mathbb{L}) \quad (17)$$

$$p_+^{(\xi)}(x, \ell) = 1_{\mathbb{L}}(\ell) p_S^{(\xi)}(x, \ell) + (1 - 1_{\mathbb{L}}(\ell)) p_B(x, \ell) \quad (18)$$

$$p_S^{(\xi)}(x, \ell) = \frac{\langle p_S(\cdot, \ell) f(x|\cdot, \ell), p^{(\xi)}(\cdot, \ell) \rangle}{\eta_S^{(\xi)}(\ell)} \quad (19)$$

$$\eta_S^{(\xi)}(\ell) = \int \langle p_S(\cdot, \ell) f(x|\cdot, \ell), p^{(\xi)}(\cdot, \ell) \rangle dx \quad (20)$$

$$w_S^{(\xi)}(L) = [\eta_S^{(\xi)}(\ell)]^L \sum_{I \subseteq \mathbb{L}} 1_I(L) [q_S^{(\xi)}]^{I-L} w^{(I, \xi)} \quad (21)$$

$$q_S^{(\xi)}(\ell) = \langle q_S(\cdot, \ell), p^{(\xi)}(\cdot, \ell) \rangle. \quad (22)$$

For a given label set,  $I_+$ , the weight  $w_+^{(I_+, \xi)}$  is a product of the weight  $w_B(I_+ \cap \mathbb{B})$  of birth labels  $I_+ - \mathbb{L} = I_+ \cap \mathbb{B}$  and the weight  $w_S^{(\xi)}(I_+ \cap \mathbb{L})$  of surviving labels  $I_+ \cap \mathbb{L}$ . The predicted single-target density for a given label  $p_+^{(\xi)}(\cdot, \ell)$  is either the

density  $p_B^{(\xi)}(\cdot, \ell)$  of a newly born target or the density  $p_S^{(\xi)}(\cdot, \ell)$  of a surviving target.

The multi-target posterior is also a  $\delta$ -GLMB with the following form

$$\pi(\mathbf{X}|Z) = \Delta(\mathbf{X}) \sum_{(I_+, \xi) \in \mathcal{F}(\mathbb{L}) \times \Xi} \sum_{\theta \in \Theta} w_+^{(I_+, \xi)} \delta_I(\mathcal{L}(\mathbf{X})) [p^{(\xi, \theta)}(\cdot|Z)]^{\mathbf{X}} \quad (23)$$

where  $\Theta$  is the space of mappings  $\theta : \mathbb{L} \rightarrow \{0, 1, \dots, |Z|\}$  such that  $\theta(i) = \theta(i') > 0$  implies  $i = i'$ , and

$$w^{(I, \xi, \theta)}(Z) = \frac{\delta_{\theta^{-1}(\{0, |Z|\})}(I) w^{(I, \xi)}[\eta_Z^{(\xi, \theta)}]^I}{\sum_{(I, \xi) \in \mathcal{F}(\mathbb{L}) \times \Xi} \sum_{\theta \in \Theta} \delta_{\theta^{-1}(\{0, |Z|\})}(I) w^{(I, \xi)}[\eta_Z^{(\xi, \theta)}]^I} \quad (24)$$

$$p^{(\xi, \theta)}(x, \ell|Z) = \frac{p^{(\xi)}(x, \ell) \psi_Z(x, \ell; \theta)}{\eta_Z^{(\xi, \theta)}(\ell)} \quad (25)$$

$$\eta_Z^{(\xi, \theta)}(\ell) = \left\langle p^{(\xi)}(\cdot, \ell), \psi_Z(\cdot, \ell; \theta) \right\rangle \quad (26)$$

$$\psi_Z(x, \ell; \theta) = \delta_0(\theta(\ell)) q_D(x, \ell) + (1 - \delta_0(\theta(\ell))) \frac{p_D(x, \ell) g(z_{\theta(\ell)}|x, \ell)}{\kappa(z)} \quad (27)$$

It is not tractable to exhaustively compute all components first and then discard those with small weights in the  $\delta$ -GLMB recursion. Hence, truncations via the ranked assignment algorithm and the K-shortest path algorithm have been proposed to find and keep components with high weights without having to propagate all the components [8]. More importantly, the truncation error can be expressed in closed form, and that truncation by keeping the highest weighted components minimizes the  $L_1$ -approximation error [8]. For this reason we adopt the GLMB filters in our algorithm.

### C. Multi-static Passive Radar Network

Tracking of multiple targets in a sensor network is a classical topic for radar, sonar and other surveillance systems. For target surveillance, passive radar systems exploit illuminators of opportunity like FM radio transmitters, digital audio/video broadcasters, WiMAX systems and global system for mobile-communication (GSM) base stations [32], [33], [34], [35]. Passive radar systems provide crucial advantages over active systems: no frequency allocation problem, receivers are hidden for a possible jamming, energy saving and much lower costs. Typically, a passive radar sensor network is realized with either one receiver and multiple transmitters or a single transmitter combined with multiple radar receivers. The latter usually costs less than the former and is studied in this paper, as shown in Fig. 1.

In passive radar networks, radar receivers may collect different kinds of target measurements, such as the time-of-arrival, direction-of-arrival, bearing, bistatic range, and Doppler shift of the reflected signals. Target-originated measurements are detected by receiver  $j$  ( $j = 1, 2, \dots, N_s$ ) with probability of detection  $p_D^{(j)}(x_k) \leq 1$ . This probability is typically a function of the distance between the target in state  $x_k$  and receiver  $j$  at location  $r^{(j)}$ . Due to the imperfect detection of receivers, false detections can also appear. The distribution of false detections over the measurement space  $\mathcal{Z}$  is assumed time invariant and

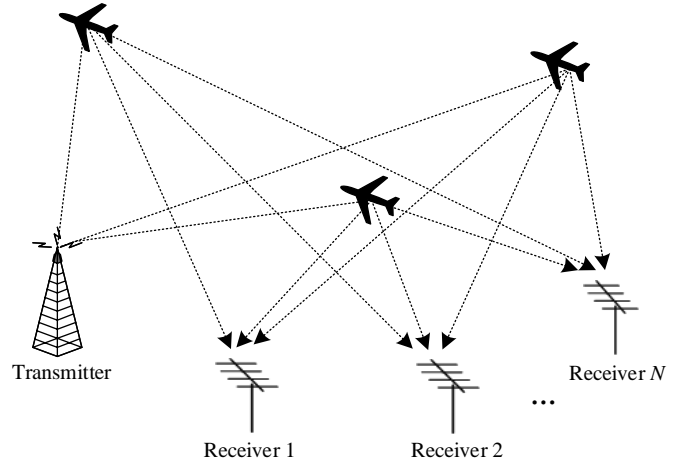


Fig. 1. Multi-target tracking using a multi-static passive radar system.

independent of target states; it will be denoted by  $c^{(j)}(z)$  for receiver  $j$ . The number of false detections per scan is assumed to be Poisson distributed, with the constant mean value  $\lambda^{(j)}$ .

At time  $k$ , the measurement set collected by sensor  $j$  is denoted as  $Z_k^{(j)} = \{z_{k,1}^{(j)}, z_{k,2}^{(j)}, \dots, z_{k,m_k^{(j)}}^{(j)}\}$ , where  $m_k^{(j)}$  is the number of measurements. It is possible that multiple sensors ‘simultaneously’ collect measurements at time  $k$ . The set of these sensors is referred to as the set of ‘activated sensors’ and is denoted as  $A_k \subseteq \{1, \dots, N_s\}$ . Measurements from all activated sensors are sent to the fusion centre for processing as they become available, in the form of messages. A message referring to measurements collected at time  $k$  has the form

$$\left( k, A_k, \cup_{j \in A_k} \left( j, Z_k^{(j)} \right) \right) \quad (28)$$

and will be denoted by  $Z_k^{(A_k)}$ .

## III. EFFICIENT SENSOR MANAGEMENT BASED ON CAUCHY-SCHWARZ DIVERGENCE

### A. Sequential Selection of Sensors

Since the number of sensors in the passive sensor network is generally large, it would be infeasible to directly use the entire information of the sensors for tracking multiple targets, and hence sensor selection is needed. Owing to the geometry, some sensors provide more informative measurements than others. The decision on which sensors should be selected can significantly affect the tracking performance. However, decisions must be made in the presence of uncertainty (both in target existence and its state) using only the past measurements. Therefore, the sensor management problem is modeled as a POMDP, as follows

$$\Psi = \{\mathbf{X}_k, \mathbb{S}, \mathbf{f}_{k|k-1}(\mathbf{X}_k|\mathbf{X}_{k-1}), g_k(Z_k|\mathbf{X}_k), \vartheta(\mathbf{X}_{k-1}, A_k, \mathbf{X}_k)\} \quad (29)$$

where  $\mathbb{S}$  denotes a finite set of sensors for selection and  $\vartheta(\mathbf{X}_{k-1}, A_k, \mathbf{X}_k)$  is an objective function that measures a reward or cost for transition from  $\mathbf{X}_{k-1}$  to  $\mathbf{X}_k$  given that the set of sensors  $A_k \subseteq \mathbb{S}$  are selected. Note that the

general formulation of a POMDP involves a  $p$ -step future decision process, whereas a single step ahead (myopic) policy is considered in this paper.

By adopting the information theoretical approach to sensor selection, the reward function is a measure of ‘information gain’ associated with each action. An optimal one-step ahead sensor selection is formulated as:

$$A_k^* = \operatorname{argmax}_{A_k \subseteq \mathbb{S}} \left\{ \mathbb{E}_{Z_k^{(A_k)}} [\vartheta(\mathbf{X}_{k-1}, A_k, \mathbf{X}_k)] \right\}. \quad (30)$$

The fact that the reward function  $\vartheta$  depends on the future measurement set  $Z_k^{(A_k)}$  is undesirable, since we want to decide on the future action without actually applying them before the decision is made. Theoretically, all possible measurement sets should be used to implement the expectation operator  $\mathbb{E}$  in (30). To reduce the computational burden, the predicted ideal measurement set (PIMS) approach [16] is used. First, the estimated number and states of targets are obtained from the predicted multi-target density. Then, a measurement is generated for each target under ideal conditions of no clutter, no measurement noise and perfect detection. Nevertheless, the computation of the reward function  $\vartheta$  can still be expensive. For the case of GLMBs, common information divergence measures such as the Kullback-Leibler or Rényi divergences [23], [24] cannot be evaluated in closed form and Monte Carlo (MC) integration is often required.

In this paper, the Cauchy-Schwarz divergence is used as the information measure, since it admits closed form expressions for Poissons [25] and GLMBs [26]. The Cauchy-Schwarz divergence between the GLMB prior density and posterior density is used as the reward function, i.e.

$$\vartheta(\mathbf{X}_{k-1}, A_k, \mathbf{X}_k) = D(\pi_k(\mathbf{X}|Z_{1:k-1}), \pi_k(\mathbf{X}|Z_{1:k-1}, Z_k^{(A_k)})) \quad (31)$$

where the prior density  $\pi_k(\mathbf{X}|Z_{1:k-1})$  is obtained by the GLMB prediction (16), and the posterior density  $\pi_k(\mathbf{X}|Z_{1:k-1}, Z_k^{(A_k)})$  is obtained using the PIMS from the sensors  $A_k$ . If we denote  $\pi_k(\mathbf{X}|Z_{1:k-1})$  and  $\pi_k(\mathbf{X}|Z_{1:k-1}, Z_k^{(A_k)})$  as

$$\pi_k(\mathbf{X}|Z_{1:k-1}) = \Delta(\mathbf{X}) \sum_{c \in \mathbb{C}} w_\phi^{(c)}(\mathcal{L}(\mathbf{X})) [p_\phi^{(c)}(\cdot)]^{\mathbf{X}} \quad (32)$$

$$\pi_k(\mathbf{X}|Z_{1:k-1}, Z_k^{(A_k)}) = \Delta(\mathbf{X}) \sum_{d \in \mathbb{D}} w_\psi^{(d)}(\mathcal{L}(\mathbf{X})) [p_\psi^{(d)}(\cdot)]^{\mathbf{X}} \quad (33)$$

respectively and assume that  $p_\phi^c$  and  $p_\psi^d$  are measured in units of  $K^{-1}$ , then the Cauchy-Schwarz divergence between

$\pi_k(\mathbf{X}|Z_{1:k-1})$  and  $\pi_k(\mathbf{X}|Z_{1:k-1}, Z_k^{(A_k)})$  is

$$D_{CS}(\pi_k(\mathbf{X}|Z_{1:k-1}), \pi_k(\mathbf{X}|Z_{1:k-1}, Z_k^{(A_k)})) = -\ln \left( \frac{\left\langle \pi_k(\mathbf{X}|Z_{1:k-1}), \pi_k(\mathbf{X}|Z_{1:k-1}, Z_k^{(A_k)}) \right\rangle_K}{\sqrt{\left\langle \pi_k(\mathbf{X}|Z_{1:k-1}), \pi_k(\mathbf{X}|Z_{1:k-1}) \right\rangle_K \times \sqrt{\left\langle \pi_k(\mathbf{X}|Z_{1:k-1}, Z_k^{(A_k)}), \pi_k(\mathbf{X}|Z_{1:k-1}, Z_k^{(A_k)}) \right\rangle_K}} \right) \quad (34)$$

where

$$\left\langle \pi_k(\mathbf{X}|Z_{1:k-1}), \pi_k(\mathbf{X}|Z_{1:k-1}, Z_k^{(A_k)}) \right\rangle_K = \sum_{L \in \mathbb{L}} \sum_{\substack{c \in \mathbb{C} \\ d \in \mathbb{D}}} w_\phi^{(c)}(L) w_\psi^{(d)}(L) \prod_{\ell \in L} K \left\langle p_\phi^{(c)}(\cdot, \ell), p_\psi^{(d)}(\cdot, \ell) \right\rangle \quad (35)$$

$$\left\langle \pi_k(\mathbf{X}|Z_{1:k-1}), \pi_k(\mathbf{X}|Z_{1:k-1}) \right\rangle_K = \sum_{L \in \mathbb{L}} \sum_{\substack{c \in \mathbb{C} \\ d \in \mathbb{C}}} w_\phi^{(c)}(L) w_\phi^{(d)}(L) \prod_{\ell \in L} K \left\langle p_\phi^{(c)}(\cdot, \ell), p_\phi^{(d)}(\cdot, \ell) \right\rangle \quad (36)$$

$$\left\langle \pi_k(\mathbf{X}|Z_{1:k-1}, Z_k^{(A_k)}), \pi_k(\mathbf{X}|Z_{1:k-1}, Z_k^{(A_k)}) \right\rangle_K = \sum_{L \in \mathbb{L}} \sum_{\substack{c \in \mathbb{D} \\ d \in \mathbb{D}}} w_\psi^{(c)}(L) w_\psi^{(d)}(L) \prod_{\ell \in L} K \left\langle p_\psi^{(c)}(\cdot, \ell), p_\psi^{(d)}(\cdot, \ell) \right\rangle. \quad (37)$$

Note that  $D_{CS}(\cdot, \cdot)$  is invariant to the unit of hyper-volume  $K$ .

Even though the reward function admits a closed form expression, finding its global optima is still intractable because searching over all possible sensor combinations is an NP-hard combinatorial optimization problem [36], [37]. We propose a suboptimal multi-sensor selection method which is computationally tractable and simple to implement. It is assumed that a fixed number  $P$  of sensors are selected at each time step, that is,  $P = |A_k| = \text{const}$ . At time  $k$ ,  $P$  sensors are selected sequentially from the candidates, as follows

$$A_k^{(j)*} = \operatorname{argmax}_{A_k^{(j)} \in \mathbb{S}} \{ \vartheta(\mathbf{X}_{k-1}, A_k^{(j)}, \mathbf{X}_k) \} \quad (38)$$

and

$$A_k^* = \bigcup_{j=1}^P A_k^{(j)*} \quad (39)$$

where  $A_k^{(j)*}$  denotes the  $j$ th selected sensor and  $\mathbb{S}$  denotes the set of remaining candidate sensors which have not been selected. The computational complexity  $\mathcal{O}(N_s)$  of the proposed approach is much smaller than searching all possible  $P$  sensor combinations in the sensor network which has complexity  $\mathcal{O}(N_s!/(N_s - P)!)$ . These two methods have the same computation burden and output if and only if  $P = 1$ .

## B. Dual-stage Sensor Fusion

For the selected sensors, the iterated-corrector multi-sensor GLMB update is used in a centralized fusion scheme, as shown in Fig. 2. The iterated-corrector multi-sensor GLMB filter consists of one predictor and multiple correctors. Compared to the single sensor case, the iterated-corrector multi-sensor filter can reduce the effect of miss detection and false alarm. It is an attractive multi-sensor algorithm due to its simple implementation and low computational complexity. However, the iterated-corrector update invariably yields different tracking results with different order of sensor updates. For example, a tracking system consists of  $P - 1$  ‘normal’ sensors and a ‘bad’ sensor with low detection ability. If the ‘bad’ sensor is the  $i$ th sensor, its negative impacts may be reduced by the later  $P - i$  sensors in the sequential update. If the ‘bad’ sensor is the last one to update, the tracking results would be poor, since there is no sensor to correct the negative impacts caused by the ‘bad’ one. In other words, the ‘bad’ sensor with a larger value of  $i$  would have more negative impact on the tracking results.

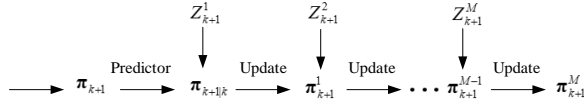


Fig. 2. Iterated-corrector multi-sensor GLMB filter with one predictor and multiple correctors.

Compared with active sensor networks, passive sensor networks have higher uncertainty. The measurements collected by passive sensor networks are typically subjected to noise corruption, missed detection, and false alarms. What’s more, the probability of detection of the passive sensor network deteriorates rapidly as the distance from the receiver increases, making multi-sensor fusion even more challenging. To address this problem, a novel dual-stage approach is developed to improve the fusion accuracy without introducing any additional computation. In the first stage, the selected sensors are ranked in increasing order of detection abilities. In the second stage, the iterated-corrector multi-sensor GLMB filter is applied according to the obtained ranking of selected sensors. The reward functions obtained in Section 3.1 are used as the ranking criterion since the value of the reward function can directly reflect the detection ability of the sensor. The sensor with minimum reward function value is updated first and the one with the maximum value is updated last. As the update progresses, the sensor with better detection ability will correct the previous result. At time step  $k$ , the pseudocode of the dual-stage fusion process is presented in Algorithm 1.

## C. Implementation

Each iteration of the GLMB filter involves an update operation and a prediction operation, both of which result in weighted sums of multi-target exponentials with intractably large number of terms. To truncate these sums and enable an efficient implementation, the ranked assignment and K-shortest path algorithms are used in the update and prediction, respectively [8]. In addition, inexpensive look-ahead strategies

## Algorithm 1 Pseudocode for a single run of the dual-stage multi-sensor GLMB fusion

**Input :**

- selected sensors:  $A_k^* = \cup_{j=1}^P A_k^{(j)*}$
- reward function  $\vartheta(\mathbf{X}_{k-1}, A_k^{(j)}, \mathbf{X}_k)$  corresponding to sensor  $A_k^{(j)*}$  ( $j = 1, \dots, P$ )
- current multi-Bernoulli density  $\pi_{k-1}(\mathbf{X}) = \Delta(\mathbf{X}) \sum_{(I, \xi) \in \mathcal{F}(\mathbb{L}) \times \Xi} w^{(I, \xi)}(\mathcal{L}(\mathbf{X})) [p^{(\xi)}]^{\mathbf{X}}$
- birth model  $\pi_{B, k}(\mathbf{X}_+) = \Delta(\mathbf{X}_+) \sum_{L \in \mathcal{F}(\mathbb{B}) \times \Xi} w_{B, k}(L) \times \delta_L(\mathcal{L}(\mathbf{X}_+)) [p_{B, k}]^{\mathbf{X}_+}$
- survival probability function  $p_S(x, \ell)$
- single-target transition density  $f(x|\cdot, \ell)$  and likelihood  $g(z|x, \ell)$
- sensor model parameters: sensor positions  $s_j = [s_x, s_y]^T$  ( $j = 1, \dots, P$ ), detection probability  $p_{D, j}(\cdot)$ , and clutter intensity  $\kappa(\cdot)$

**Output :**

→ the fused posterior density to be propagated to next time, parameterized by  $\{\tilde{r}^{(\ell)}, \{\tilde{w}_j^{(\ell)}, \tilde{x}_j^{(\ell)}\}_{j=1}^J, \tilde{J}^{(\ell)}\}_{\ell \in \mathbb{L}}$

**Step 1 :** Rank the selected sensors  $A_k^*$  in order of the value of the reward function  $\vartheta(\mathbf{X}_{k-1}, A_k^{(j)}, \mathbf{X}_k)$  ( $j = 1, \dots, P$ ) from small to large

**Step 2 :** Iterated-corrector multi-sensor GLMB fusion

- 1) **for** sensor  $j \in A_k^*$  **do**
- 2) **if**  $j = 1$  **do**
- 3) Predict the prior  $\delta$ -GLMB using (16)-(22) to obtain the multi-target prediction  $\pi_+^{(j)} = \Delta(\mathbf{X}_+) \sum_{(I, \xi) \in \mathcal{F}(\mathbb{L}_+) \times \Xi} w_+^{(I, \xi)} \times \delta_{I_+}(\mathcal{L}(\mathbf{X}_+)) [p_+^{(\xi)}]^{\mathbf{X}_+}$
- 4) **else do**
- 5) Pseudo-predict  $\pi_+^{(j)} = \pi^{(j-1)}(\mathbf{X}|Z)$
- 6) **end if**
- 7) Update the predicted  $\delta$ -GLMB using (23)-(27) to obtain the multi-target posterior  $\pi^{(j)}(\mathbf{X}|Z) = \Delta(\mathbf{X}) \sum_{(I, \xi) \in \mathcal{F}(\mathbb{L}) \times \Xi} \sum_{\theta \in \Theta} w^{(I, \xi)} \times \delta_I(\mathcal{L}(\mathbf{X})) [p^{(\xi, \theta)}(\cdot|Z)]^{\mathbf{X}}$
- 8) **end for**
- 9) The fused posterior  $\pi(\mathbf{X}|Z) = \pi^{(j)}(\mathbf{X}|Z)$

can be adopted to reduce the number of computations [8]. There are two implementations of the GLMB recursion: one is using Gaussian mixtures (GMs) and the other is using sequential Monte Carlo (SMC) method. For a linear Gaussian multi-target model (with constant survival and detection probabilities), each relevant single target density  $p_{k-1}^{(\xi)}(\cdot, \ell)$  is represented as a GM, and the predicted and updated densities  $p_{k|k-1}^{(\xi)}(\cdot, \ell)$ ,  $p_k^{(\xi)}(\cdot, \ell)$  are computed using the standard GM update and prediction formulas based on the Kalman filter. For non-linear non-Gaussian multi-target models (with state dependent survival and detection probabilities), each single target density  $p_{k-1}^{(\xi)}(\cdot, \ell)$  is represented by a set of weighted particles. The corresponding predicted and updated densities  $p_{k|k-1}^{(\xi)}(\cdot, \ell)$ ,  $p_k^{(\xi, \theta)}(\cdot, \ell)$  are computed by the SMC method. In this paper, the SMC implementation is adopted to handle the nonlinear dynamic and measurement models, and also the state-dependent probability of detection.

Starting with a GLMB prior (which is the fused GLMB posterior from previous time), GLMB filtering is implemented in conjunction with an efficient sensor selection (ESS) and dual-stage fusion (DSF). A general schematic diagram for a complete run of the proposed ESS-DFS-GLMB filter is shown in Fig. 3.

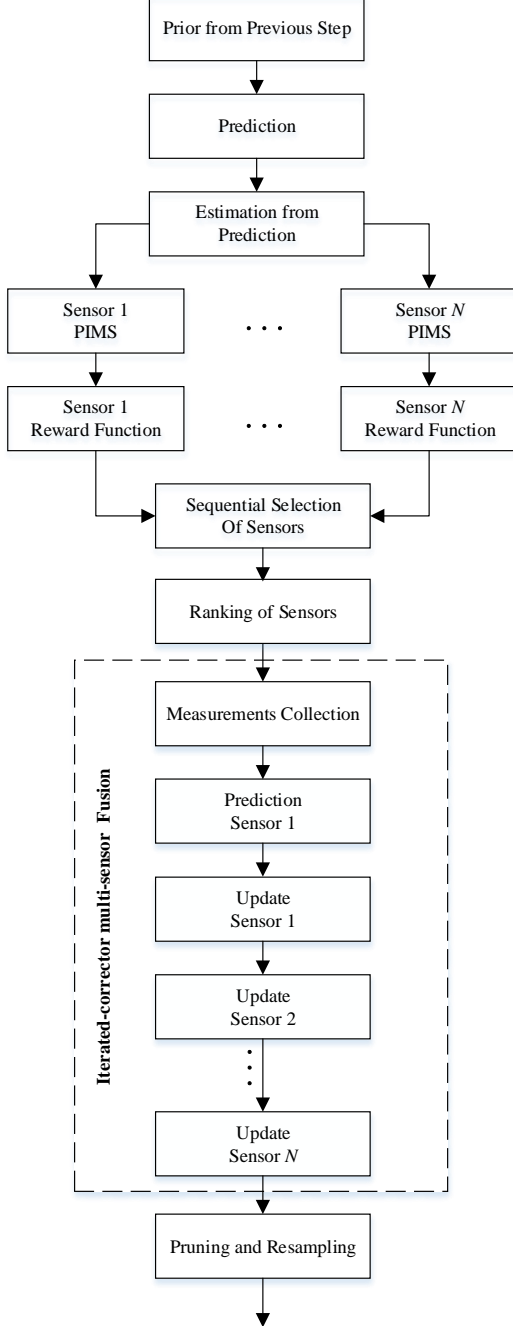


Fig. 3. Schematic diagram of the ESS-DFS-GLMB filter.

#### IV. SIMULATIONS

Two challenging scenarios are used to study the performance of the proposed ESS-DFS-GLMB filter in a passive sensor network. Bistatic range (transmitter-target-receiver) and bearing measurements are used. In Scenario 1, a total number

of three targets with non-linear motions move through the surveillance area and in close proximity to each other. In Scenario 2, a more challenging multi-target tracking problem is considered. The total number of targets is increased into six, and locations of targets are relatively scattered. The scattered distribution of the targets makes it impossible to intuitively obtain the optimal selection solution and will increase the difficulty of sensor management. The structure of the passive sensor network is borrowed from [38], where one transmitter and ten receivers are placed in the  $x$ - $y$  plane as shown in Fig. 4(a). During the target tracking process,  $P$  receivers are selected automatically at each time step. The probability of detection is modeled as follows [38]

$$p_D^{(j)}(x_k) = 1 - \phi(\|p_k - r^j\|; \alpha, \beta) \quad (40)$$

where  $p_k = [x_k, y_k]^T$  is the target position,  $r^j = [x_R^j, y_R^j]^T$  is the position of receiver  $j$ ,  $d_{k,j} = \|p_k - r^j\|$  is the distance between the target and the receiver, and  $\phi(d; \alpha, \beta) = \int_{-\infty}^d \mathcal{N}(v; \alpha, \beta) dv$  is the Gaussian cumulative distribution function with  $\alpha = 15$  km and  $\beta = (4 \text{ km})^2$ . Fig. 4(b) plots the probability of detection as a function of the distance between the receiver and the target. As the distance from the receiver increases, the probability of detection of the passive sensor decreases quickly [39]. The poor detection ability makes the sensor management problem for target tracking difficult, and many state-of-the-art techniques would fail.

If a target located at  $p_k = [x_k, y_k]^T$  is detected by receiver  $j$ , then the target-originated measurement is a noisy bearing and bistatic range (transmitter-target-receiver) vector given by

$$z_k^j = \begin{bmatrix} \varphi^j \\ \rho^j \end{bmatrix} = \begin{bmatrix} \arctan\left(\frac{y_k - y_R^j}{x_k - x_R^j}\right) \\ \frac{\sqrt{(x_k - x_T)^2 + (y_k - y_T)^2}}{\sqrt{(x_k - x_R^j)^2 + (y_k - y_R^j)^2}} \end{bmatrix} + \varepsilon_k^j \quad (41)$$

where  $t = [x_T, y_T]^T$  is the location of the transmitter and  $\varepsilon_k^j \sim \mathcal{N}(0; 0, R_k^j)$  with  $R_k^j = \text{diag}([\sigma_\varphi^2, \sigma_\rho^2])$ . The scales of measurement noise are given by:  $\sigma_\varphi = \varphi_0 + \eta_\varphi \|r^j - p_k\|$ ;  $\sigma_\rho = \rho_0 + \eta_\rho \|r^j - p_k\|^2$ , in which  $\|r^j - p_k\|^2 = (x_R^j - x_k)^2 + (y_R^j - y_k)^2$ ,  $\rho_0 = 1\text{m}$ ,  $\eta_\rho = 5 \times 10^{-5} \text{ m}^{-1}$ ,  $\varphi_0 = \pi/180$  rad, and  $\eta_\varphi = 1 \times 10^{-5} \text{ m}^{-1}$ . The geometry of a single transmitter-target-receiver pair is illustrated in Fig. 5, where locations of the transmitter, receiver and target are denoted as  $(x_T, y_T)$ ,  $(x_R, y_R)$  and  $(x, y)$ , respectively. Clutter measurements for each receiver are distributed uniformly over the region  $[-\pi, \pi] \text{ rad} \times [0, 15000] \text{ m}$ . The number of clutter measurements per scan is assumed to be Poisson distributed with the clutter intensity  $\lambda_c = 2 \times 10^{-5} (\text{radm})^{-1}$ . Without loss of generality, the tracking performance of the proposed RFS-based approach is evaluated using the OSPA error distance [40], in which the order parameter  $p$  determines the sensitivity to outliers and the cut-off parameter  $c$  determines the relative weighting of the penalties assigned to cardinality and localization errors. For each scenario, the average error performances are obtained over 50 MC trials. All experiments

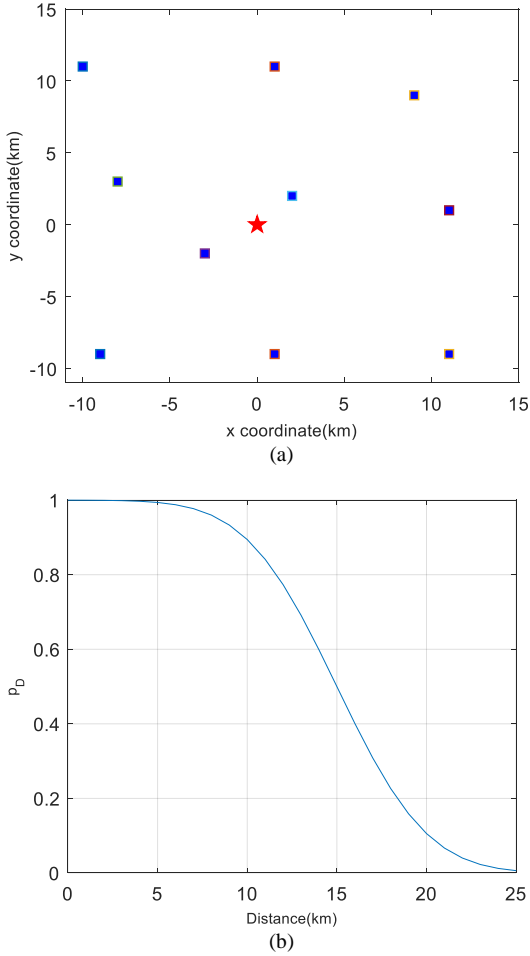


Fig. 4. System setup: (a) The locations of receivers (squares) and the transmitter (star); (b) Probability of detection as a function of the distance from a receiver.

are tested in Matlab R2010a and implemented on a computer with a 3.40 GHz processor.

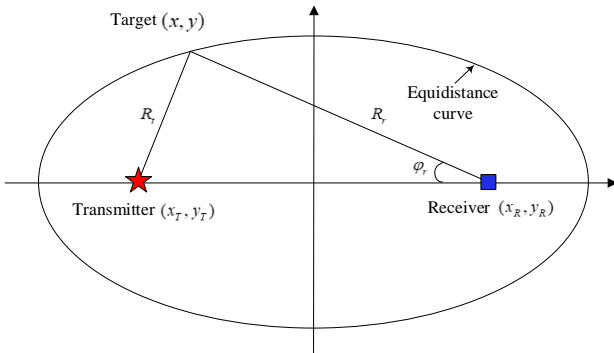


Fig. 5. The geometry of a single transmitter-target-receiver pair. The equidistance curve can be plotted using the bistatic range  $\rho = R_t + R_r$  and the target position is further determined using the bearing  $\varphi_r$ .

#### A. Scenario 1

In this scenario, a nearly constant turn model is considered. The target state is denoted as  $x_k = [\tilde{x}_k^T, \omega_k^T]^T$  where  $\tilde{x}_k =$

$[x_k, \dot{x}_k, y_k, \dot{y}_k]^T$  comprises the target position and velocity and  $\omega_k$  is the turn rate. The state transition model is

$$\tilde{x}_k = F(\omega_{k-1})\tilde{x}_{k-1} + G\omega_{k-1}$$

where

$$F(\omega_{k-1}) = \begin{bmatrix} 1 & \frac{\sin \omega T_s}{\omega} & 0 & -\frac{1 - \cos \omega T_s}{\omega} \\ 0 & \cos \omega T_s & 0 & -\sin \omega T_s \\ 0 & \frac{1 - \cos \omega T_s}{\omega} & 1 & \frac{\sin \omega T_s}{\omega} \\ 0 & \sin \omega T_s & 0 & \cos \omega T_s \end{bmatrix}$$

$$G = \begin{bmatrix} \frac{T_s^2}{2} & 0 \\ T_s & 0 \\ 0 & \frac{T_s^2}{2} \\ 0 & T_s \end{bmatrix}$$

and  $\omega_{k-1} \sim \mathcal{N}(0; 0, Q)$  is a 2D independent and identically distributed Gaussian process noise vector with covariance  $Q = \sigma_\omega^2 I_2$ , where  $\sigma_\omega = 0.01 \text{ m/s}^2$  is the standard deviation of the target acceleration. The sampling interval is fixed to  $T_s = 10 \text{ s}$ . A total of three targets appear in the surveillance area and the true trajectories of targets are shown in Fig. 6, in which Target 1 is born at  $k = 1$ , Target 2 is born at  $k = 10$ , and Target 3 is born at  $k = 20$ .

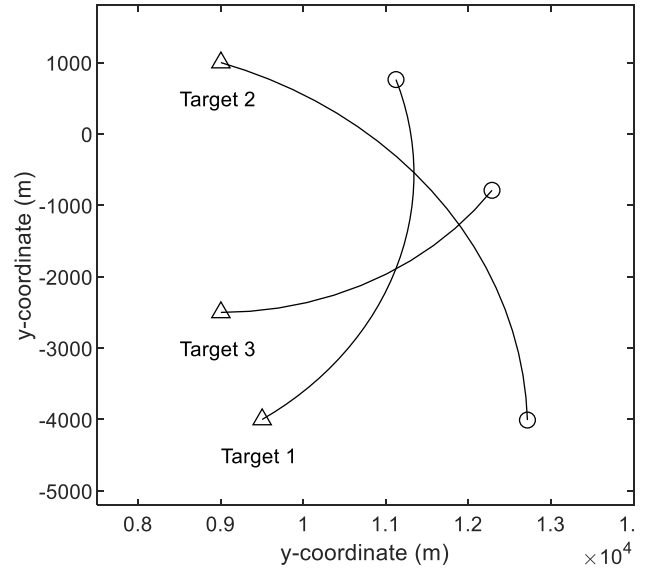


Fig. 6. Target trajectories of Scenario 1 in the  $x/y$  plane. Start/Stop positions for each track are shown with  $\circ / \Delta$ .

The birth process is a labeled multi-Bernoulli RFS with parameters  $f_B(x) = \{w_B, p_B^{(i)}\}_{i=1}^3$ , where the common existence probabilities  $w_B = 0.02$ , and  $p_B^{(i)}(x) = \mathcal{N}(x; m_B^{(i)}, P_B)$  with  $m_B^{(1)} = [9500, 0, -4000, 0, 0]^T$ ,  $m_B^{(2)} = [9000, 0, 1000, 0, 0]^T$ ,  $m_B^{(3)} = [9000, 0, -2500, 0, 0]^T$ , and  $P_B = \text{diag}([100, 10, 100, 10, \pi/180])^2$ . The units are meters for  $x$  and  $y$  and meters per second for  $\dot{x}$  and  $\dot{y}$ . At each time step,  $L = 3000$  particles per birth track is imposed. The number of components calculated and stored in each forward propagation is set to be 1000. The survival probability is fixed to  $p_s = 0.99$ . The ESS-DFS-GLMB filter output for a single



MC run for the case where the number of sensors selected at each time step  $k$  is fixed to  $P = |A_k| = 2$ , is given in Fig. 7, showing the true and estimated tracks in  $x$  and  $y$  coordinates versus time. The plots indicate that the ESS-DFS-GLMB filter is able to identify all target births, as well as successfully accommodating nonlinearities.

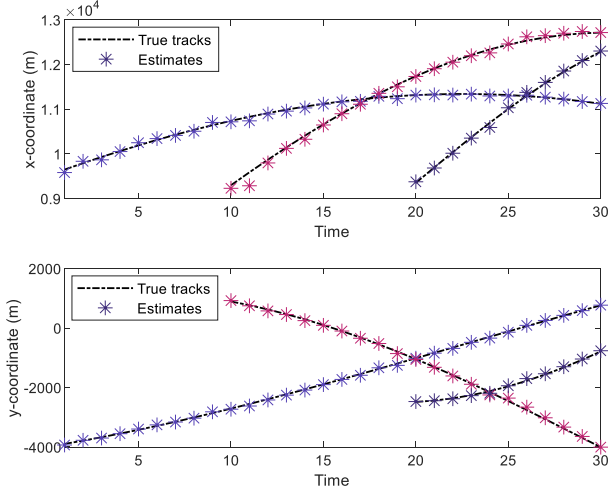


Fig. 7. True and estimated tracks versus time in Scenario 1.

To evaluate the performance of the ESS-DFS-GLMB filter, we compare it with the heuristic random selection method, the exhaustive search scheme, and the ESS-GLMB filter. In the random selection method,  $P$  sensors are selected randomly at each time step and it is assumed that each sensor has an equal probability to be chosen. In the exhaustive search scheme, the Cauchy-Schwarz divergence is computed for all possible combinations of  $P$  sensors in the network and is used to solve the optimization problem. In order to have an optimal solution, the order of sensors is taken into account in the exhaustive search scheme. To validate the performance of the dual-stage multi-sensor fusion in the ESS-DFS-GLMB filter, the ESS-GLMB filter is also used as a benchmark in which sensors are selected using the proposed efficient selection method but measurements from selected sensors are updated in a random order. To make the comparisons more meaningful, the PIMS strategy is taken by all of the above methods.

The MC averages of the OSPA distance (for  $p = 1$ ,  $c = 200$  m) for two and three sensors selected at each time step are given in Fig. 8(a) and (b), respectively. It can be observed that the ESS-DFS-GLMB filter performs better than the random selection method and the ESS-GLMB filter. In passive sensor networks, the probability of detection of the passive sensor decreases quickly the distance from the receiver increases. Therefore, the detection abilities of sensors vary considerably with moving of targets. In this case, the proposed dual-step multi-sensor fusion is a good choice to improve the multi-sensor fusion results. Fig. 8 also demonstrates that in terms of multi-target tracking errors, the ESS-DFS-GLMB filter is even comparable with the state of art.

To compare the computational efficiencies of the ESS-DFS-GLMB filter and the exhaustive search scheme, the average computing time (in sec) for each method to execute a complete

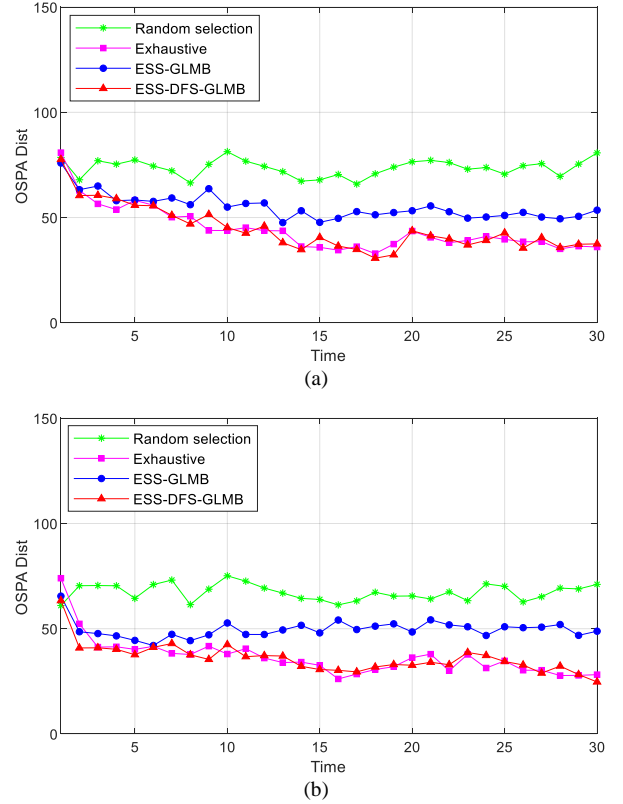


Fig. 8. Average OSPA errors in Scenario 1: (a)  $P = 2$ ; (b)  $P = 3$ .

MC simulation against different number  $P$  of selected sensors is shown in Table 1. As seen from Table 1, there is an overall increase of the computing time with the increase of  $P$ . When  $P = 1$ , the computing time of the exhaustive search scheme and the ESS-DFS-GLMB method is comparable with each other. As mentioned before, when  $P = 1$ , these two methods degenerate into the same sensor management solution. The ESS-DFS-GLMB filter runs about 13.45 times faster than the exhaustive search method when  $P = 2$ , and 137.33 times faster when  $P = 3$ . These results are good agreement with the theoretical analysis of the computational complexity.

TABLE I  
COMPUTING TIME COMPARISON FOR SCENARIO 1 (s)

| Number of selected sensors | Exhaustive | ESS-DFS-GLMB |
|----------------------------|------------|--------------|
| $P = 1$                    | 181.45     | 176.72       |
| $P = 2$                    | 3908.18    | 290.47       |
| $P = 3$                    | 52161.40   | 379.83       |

## B. Scenario 2

We now consider a more complicated scenario and assume a total number of six targets in the surveillance area. The target state variable is a vector of target position and velocity and is denoted as  $x_k = [x_k, y_k, \dot{x}_k, \dot{y}_k]$ . The single-target transition model is linear Gaussian specified by

$$x_k = F_k x_{k-1} + u_k$$

with the transition matrix

$$F_k = \begin{bmatrix} 1 & 0 & T_s & 0 \\ 0 & 1 & 0 & T_s \\ 0 & 0 & 1 & 0 \\ 0 & 0 & 0 & 1 \end{bmatrix}.$$

The process noise is zero-mean Gaussian distributed with covariance

$$Q = \sigma_u^2 \begin{bmatrix} \frac{T_s^3}{3} & 0 & \frac{T_s^2}{2} & 0 \\ 0 & \frac{T_s^3}{3} & 0 & \frac{T_s^2}{2} \\ \frac{T_s^2}{2} & 0 & T_s & 0 \\ 0 & \frac{T_s^2}{2} & 0 & T_s \end{bmatrix}$$

where  $\sigma_u = 0.01 \text{ m/s}^2$  is the standard deviation of the process noise. The true trajectories are shown in Fig. 9, in which Target 1 is born at  $k = 1$ , Targets 2 is born at  $k = 10$ , Targets 3 and 6 are born at  $k = 20$ , and Targets 4 and 5 are born at  $k = 15$ .

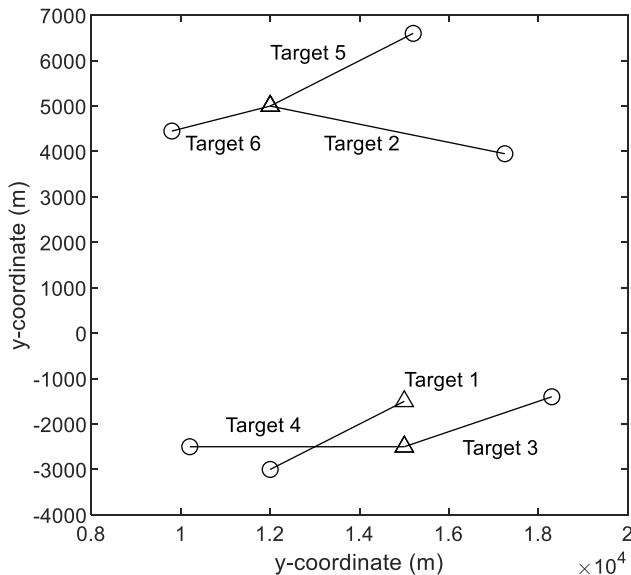


Fig. 9. Target trajectories of Scenario 2 in the  $x/y$  plane. Start/Stop positions for each track are shown with  $\circ/\Delta$ .

The birth process is a labeled multi-Bernoulli RFS with parameters  $f_B(x) = \{w_B, p_B^{(i)}\}_{i=1}^3$ , where the common existence probabilities  $w_B = 0.02$ , and  $p_B^{(i)}(x) = \mathcal{N}(x; m_B^{(i)}, P_B)$  with  $m_B^{(1)} = [15000, 0, -1500, 0]^T$ ,  $m_B^{(2)} = [12000, 0, 5000, 0]^T$ ,  $m_B^{(3)} = [15000, 0, -2500, 0]^T$ , and  $P_B = \text{diag}([100, 10, 100, 10]^T)^2$ . All other parameters are the same as those in the previous scenario. The ESS-DFS-GLMB filter output for a single MC run for the case where the number of sensors selected at each time step  $k$  is fixed to  $P = |A_k| = 2$ , is given in Fig. 10, showing the true and estimated tracks in  $x$  and  $y$  coordinates versus time. The results suggest that the trajectory estimates are very close to the true target trajectories.

The MC averages of the OSPA distance (for  $p = 1$ ,  $c = 200 \text{ m}$ ) for two and three sensors selected at each time step are given in Fig. 11(a) and (b), respectively. When  $P=3$ , the computing burden of the exhaustive search scheme is overload and hence it is not considered here. It can be observed from Fig. 11 that the ESS-DFS-GLMB filter performs better than

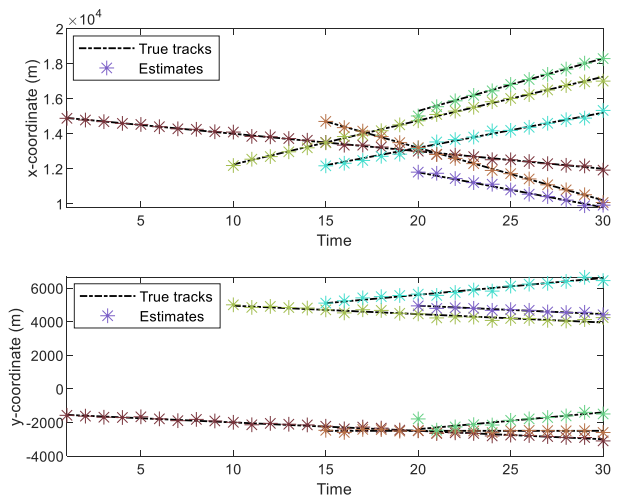


Fig. 10. True and estimated tracks versus time in Scenario 2.

the random selection method and the ESS-GLMB filter. When  $P = 2$ , the tracking accuracy of the ESS-DFS-GLMB filter and the optimal exhaustive search scheme is comparable with each other.

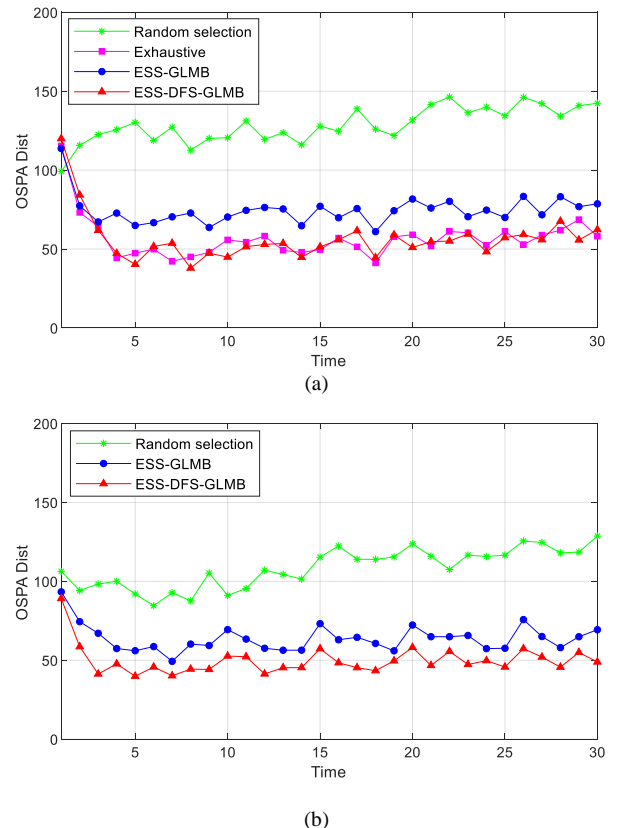


Fig. 11. Average OSPA errors in scenario 2 (a)  $P = 2$ ; (b)  $P = 3$ .

To compare the computational efficiencies of the ESS-DFS-GLMB filter and the exhaustive search scheme, the average computing time (in sec) for each method to execute a complete MC simulation against different number  $P$  of selected sensors is shown in Table 2. The computing time of the exhaustive

method and the ESS-DFS-GLMB filter is comparable with each other when  $P = 1$ . The ESS-DFS-GLMB filter runs about 16.89 times faster than the exhaustive search method when  $P = 2$ .

TABLE II  
COMPUTING TIME COMPARISON FOR SCENARIO 2 (S)

| Number of selected sensors | Exhaustive | ESS-DFS-GLMB |
|----------------------------|------------|--------------|
| $P = 1$                    | 301.49     | 289.71       |
| $P = 2$                    | 9349.23    | 553.47       |
| $P = 3$                    | Overload   | 792.10       |

## V. CONCLUSIONS

An efficient sensor management approach named ESS-DFS-GLMB has been proposed in this paper for multi-target tracking in passive sensor networks. Since the number of sensors in passive sensor networks is generally large, it would not be feasible to directly use the information on the entire sensor collection and hence the need for sensor selection. However, the sensor selection is a global combinatorial optimization problem that is extremely challenging when the network is large. To solve this problem, an efficient information-theoretic sensor selection strategy has been developed using the GLMB filter. At each time step, a fixed number of sensors are selected sequentially from the candidates based on the Cauchy-Schwarz divergence. For the selected sensors, the iterated-corrector multi-sensor GLMB filter is applied sequentially in an order determined by their Cauchy-Schwarz divergences. This so-called proposed dual-stage sequential update scheme well improves the fusion accuracy without introducing any additional computation.

Numerical studies are presented for two challenging scenarios where multiple moving targets are to be tracked in a passive sensor network using non-linear measurements. The results demonstrate the superior tracking accuracy of the ESS-DFS-GLMB approach in terms of OSPA errors. What's more, the computing time comparison results show that it runs substantially faster than the exhaustive search-based technique. These results are good agreement with the theoretical analysis of the computational complexity. Future work will consider the learning of clutter statistics and integration of data over multiple scans [12] to improve tracking performance.

## REFERENCES

- [1] S. Joshi and S. Boyd, "Sensor selection via convex optimization," *IEEE Trans. Signal Process.*, vol. 57, no. 2, pp. 451–462, 2009.
- [2] J. Yick, B. Mukherjee, and D. Ghosal, "Wireless sensor network survey," *Comput. Netw.*, vol. 52, no. 12, pp. 2292–2330, 2008.
- [3] R. Mahler, *Statistical Multisource-Multitarget Information Fusion*. Norwood, MA: Artech House, 2007.
- [4] R. Mahler, "Multi-target Bayes filtering via first-order multi-target moments," *IEEE Trans. Aerosp. Electron. Syst.*, vol. 39, no. 4, pp. 1152–1178, 2003.
- [5] R. Mahler, "PHD filters of higher order in target number," *IEEE Trans. Aerosp. Electron. Syst.*, vol. 43, no. 4, pp. 1523–1543, 2007.
- [6] B.-T. Vo, B.-N. Vo, and A. Cantoni, "The cardinality balanced multi-target multi-Bernoulli filter and its implementations," *IEEE Trans. Signal Process.*, vol. 57, no. 2, pp. 409–423, 2009.
- [7] B.-T. Vo and B.-N. Vo, "Labeled random finite sets and multi-target conjugate priors," *IEEE Trans. Signal Process.*, vol. 61, no. 13, pp. 3460–3475, 2013.
- [8] B.-N. Vo, B.-T. Vo, and D. Phung, "Labeled random finite sets and the Bayes multi-target tracking filter," *IEEE Trans. Signal Process.*, vol. 62, no. 24, pp. 6554–6567, 2014.
- [9] B.-N. Vo, B.-T. Vo, and H. G. Hoang, "An efficient implementation of the generalized labeled multi-Bernoulli filter," *IEEE Trans. Signal Process.*, vol. 65, no. 8, pp. 1975–1987, 2017.
- [10] M. Beard, B.-T. Vo, and B.-N. Vo, "A solution for large-scale multi-object tracking," *IEEE Trans. Signal Process.*, vol. 68, pp. 2754–2769, 2020.
- [11] B.-N. Vo, B.-T. Vo, and M. Beard, "Multi-sensor multi-object tracking with the generalized labeled multi-Bernoulli filter," *IEEE Trans. Signal Process.*, vol. 67, no. 23, pp. 5952–5967, 2019.
- [12] B.-N. Vo and B.-T. Vo, "Multi-scan generalized labeled multi-Bernoulli models for multi-object state estimation," *IEEE Trans. Signal Process.*, vol. 67, no. 19, pp. 4998–4963, 2019.
- [13] H. G. Hoang and B.-T. Vo, "Sensor management for multi-target tracking via multi-Bernoulli filtering," *Automatica*, vol. 50, no. 4, pp. 1135–1142, 2014.
- [14] A. K. Gostar, R. Hoseinnezhad, and A. Bab-Hadiashar, "Multi-Bernoulli sensor control for multi-target tracking," in *Proc. Int. Con. Intelligent. Sensors, Sensor Networks and Information Processing (ISSNIP 2013)*, Melbourne, Australia, 2013, pp. 312–317.
- [15] A. K. Gostar, R. Hoseinnezhad, and A. Bab-Hadiashar, "Multi-Bernoulli sensor control via minimization of expected estimation errors," *IEEE Trans. Aerosp. Electron. Syst.*, vol. 51, no. 3, pp. 1762–1773, 2015.
- [16] R. Mahler, "Multitarget sensor management of dispersed mobile sensors," in *Theory and Algorithms for Cooperative Systems*, D. Grunzel, R. Murphey, and P. Pardalos, Eds. Singapore: World Scientific, 2004, pp. 239–310.
- [17] R. Mahler, "Sensor management with non-ideal sensor dynamics," in *Proc. 7th Int. Conf. Information Fusion*, Stockholm, Sweden, 2004, pp. 1–8.
- [18] R. Mahler, "Unified sensor management using CPHD filters," in *Proc. 10th Int. Conf. Information Fusion*, Quebec City, Canada, 2007, pp. 1–7.
- [19] A. K. Gostar, R. Hoseinnezhad, and A. Bab-Hadiashar, "Robust multi-Bernoulli sensor selection for multi-target tracking in sensor networks," *IEEE Signal Process. Lett.*, vol. 20, no. 12, pp. 1167–1170, 2013.
- [20] A. K. Gostar, R. Hoseinnezhad, and A. Bab-Hadiashar, "Multi-Bernoulli sensor-selection for multi-target tracking with unknown clutter and detection profiles," *Signal Process.*, vol. 119, pp. 28–42, 2016.
- [21] A. K. Gostar, R. Hoseinnezhad, and A. Bab-Hadiashar, "Sensor control for multi-object tracking using labeled multi-Bernoulli filter," in *Proc. Int. Conf. Information Fusion*, Salamanca, 2014, pp. 1–8.
- [22] Y. Zhu, J. Wang, and S. Liang, "Multi-objective optimization based multi-Bernoulli sensor selection for multi-target tracking," *Sensors*, vol. 19, no. 4, pp. 1–18, 2019.
- [23] R. Mahler, "Global posterior densities for sensor management," in *Proc. International Society for Optics and Photonics*, Orlando, USA, 1998, pp. 252–263.
- [24] B. Ristic and B.-N. Vo, "Sensor control for multi-object state-space estimation using random finite sets," *Automatica*, vol. 46, no. 11, pp. 1812–1818, 2010.
- [25] H. G. Hoang, B.-N. Vo, B.-T. Vo, and R. Mahler, "The Cauchy-Schwarz divergence for Poisson point processes," *IEEE Trans. Information Theory*, vol. 61, no. 8, pp. 4475–4485, 2015.
- [26] M. Beard, B.-T. Vo, B.-N. Vo, and S. Arulampalam, "Void probabilities and Cauchy-Schwarz divergence for generalized labeled multi-Bernoulli models," *IEEE Trans. Signal Process.*, vol. 65, no. 19, pp. 5047–5061, 2017.
- [27] H. V. Nguyen, H. Rezaatofghi, B.-N. Vo, and D. Ranasinghe, "Online UAV path planning for joint detection and tracking of multiple radio-tagged objects," *IEEE Trans. Signal Process.*, vol. 67, no. 20, pp. 5365–5379, 2019.
- [28] H. V. Nguyen, H. Rezaatofghi, B.-N. Vo, and D. Ranasinghe, "Multi-objective multi-agent planning for jointly discovering and tracking mobile object," in *Proc. AAAI Conference on Artificial Intelligence*, New York, USA, 2020, pp. 7227–7235.
- [29] L. Ma, K. Xue, and P. Wang, "Multitarget tracking with spatial nonmaximum suppressed sensor selection," *Mathematical Problems in Engineering*, vol. 4, pp. 1–10, 2015.
- [30] L. Ma, K. Xue, and P. Wang, "Distributed multiagent control approach for multitarget tracking," *Mathematical Problems in Engineering*, vol. 1, pp. 1–10, 2015.
- [31] P. Wang, L. Ma, and K. Xue, "Multitarget tracking in sensor networks via efficient information-theoretic sensor selection," *International Journal of Advanced Robotic Systems*, vol. 14, no. 5, pp. 1–9, 2017.

- [32] H. D. Griffiths and C. J. Baker, "Passive coherent location radar systems. Part 1: Performance prediction," *IET Radar Sonar and Navigation*, vol. 3, no. 152, pp. 153–159, 2005.
- [33] K. Chetty, K. Woodbridge, H. Guo, and G. Smith, "Passive bistatic WiMAX radar for marine surveillance," in *IEEE Radar Conference*, Washington, DC, USA, 2010, pp. 188–193.
- [34] M. Daun and U. Nickel, "Tracking in multistatic passive radar systems using DAB/DVB-T illumination," *Signal Process.*, vol. 92, no. 6, pp. 1365–1386, 2012.
- [35] D. K. P. Tan, H. Sun, Y. Lu, M. Lesturgie, and H. L. Chan, "Passive radar using global system for mobile communication signal: Theory, implementation and measurements," *IET Radar Sonar and Navigation*, vol. 3, no. 152, pp. 116–123, 2005.
- [36] T. S. Yoo and S. Lafortune, "NP-completeness of sensor selection problems arising in partially observed discrete-event systems," *IEEE Trans. Autom. Control*, vol. 47, no. 9, p. 1495–1499, 2002.
- [37] F. Bian, D. Kempe, and R. Govindan, "Utility based sensor selection," in *Proc. 5th Int. Conf. Information Processing in Sensor Networks*, New York, USA, 2006, pp. 11–18.
- [38] B. Ristic and A. Farina, "Target tracking via multi-static Doppler shifts," *IET Radar Sonar and Navigation*, vol. 7, no. 5, pp. 508–516, 2013.
- [39] B. R. Mahafza, *Radar systems analysis and design using MATLAB, 3rd ed.* Boca Raton, Florida, USA: Chapman and Hall/CRC Press., 2013.
- [40] D. Schuhmacher, B.-T. Vo, and B.-N. Vo, "A consistent metric for performance evaluation of multi-object filters," *IEEE Trans. Signal Process.*, vol. 56, no. 8, pp. 3447–3457, 2008.